



# Cerium Doped Pt/TiO<sub>2</sub> for Catalytic Oxidation of Low Concentration Formaldehyde at Room Temperature

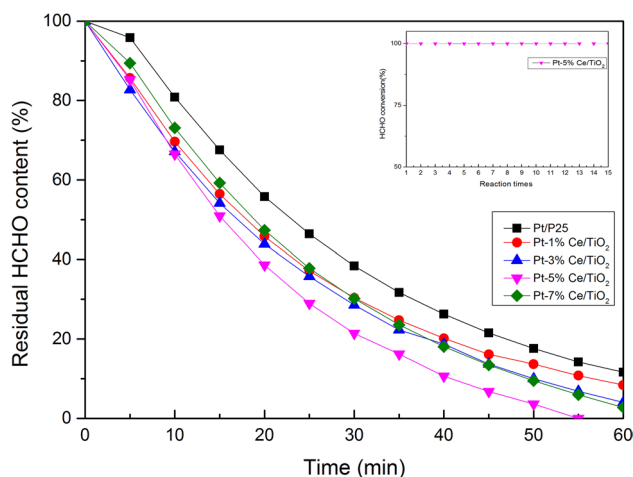
Yuanyuan Shi<sup>1</sup> · Zhiwei Qiao<sup>1</sup> · Zili Liu<sup>1</sup> · Jianliang Zuo<sup>1</sup>

Received: 3 October 2018 / Accepted: 30 December 2018 / Published online: 20 February 2019  
© Springer Science+Business Media, LLC, part of Springer Nature 2019

## Abstract

Formaldehyde is a carcinogenic and teratogenic toxic gas. With the extensive use of a variety of building materials, indoor formaldehyde has seriously threatened human health and environment. The catalytic oxidation is considered the most promising method for the removal of formaldehyde from air. In this work, we report a Pt/TiO<sub>2</sub> catalyst with Ce modification, and investigate its activity of catalytic oxidation of low concentration formaldehyde at room temperature. The experimental results show that the trace formaldehyde (20 mg/m<sup>3</sup>) could be completely degraded at 55 min by using Pt–Ce/TiO<sub>2</sub> catalyst. In view of multiple characterizations, such as BET, XRD, TEM, STEM, XPS and CO adsorption, it is indicated that the modification of Ce can effectively improve the dispersion of Pt particles in the surface and reduction of Pt particle size from 2.9 to 2.2 nm. Moreover, XPS results show that the Ce in the catalyst could enhance the binding energies of Pt, provide abundant oxygen vacancies, and could increase the ratio of adsorbed oxygen atoms to lattice oxygen atoms, which is conducive to the adsorption of oxygen, leading to the improvement of catalytic activity.

## Graphical Abstract



**Keywords** Low concentration formaldehyde · Room temperature · Platinum · Titania · Ce modification

## 1 Introduction

Formaldehyde (HCHO) is a kind of colorless poisonous gas with strong pungent odor, the main source of indoor formaldehyde is interior decoration materials, such as artificial synthesis plank, emulsion paint, carpet fabric and resin decorations and furniture. The formaldehyde can be slowly

✉ Zili Liu  
gzdxlzl@gmail.com

Extended author information available on the last page of the article

released from the materials, and the release period could exceed by 3–15 years, leading to the concentration of formaldehyde in the house keeping higher than the outside [1]. Prolonged exposure to low concentrations of formaldehyde can cause chronic respiratory diseases, chromosomal abnormalities, and even nasopharyngeal cancer or fetal malformation. The eliminating indoor formaldehyde from the source is unable to be achieved perfectly at present, thus the removal of indoor formaldehyde is widely paid attention by many researchers. In recent years, the techniques for removing the indoor formaldehyde mainly include adsorption [2, 3], plant purification, plasma technique [4], photocatalytic oxidation technique [5, 6] and catalytic oxidation technique [7–9]. The catalytic oxidation technique has no secondary pollution with advantages of high efficiency, complete treatment and extremely effective treatment for low concentration formaldehyde. Therefore, the catalytic oxidation is considered to be the most promising and effective technique to remove formaldehyde from indoor air.

In the past decades, the technology of catalytic oxidation to remove formaldehyde has made considerable progress [10–13]. At present, the precious metal catalysts used in the catalytic oxidation of formaldehyde mainly included Pt, Au, Pd, Ag, Ru etc [8, 9, 14–16]. While, due to very high conversion rate and long life of catalytic oxidation of formaldehyde under low temperature, the Pt-supported catalyst has been paid attention by most of researchers. In the preparation of supported precious metal catalyst, the support plays an important role for its activity, and the choice of different supports has important influence on the dispersion and size of loaded precious metal particles. Besides, the activity of catalyst is also reflected in the numbers of oxygen vacancy and the interactions between the supports and precious metals. Yan et al. [17] used the combination of AlOOH and CeO<sub>2</sub> as the carrier to support the noble metal platinum. The catalyst showed an excellent activity and stability for the catalytic oxidation of formaldehyde at room temperature, the main reason is the rich hydroxyl groups on the surface of CeO<sub>2</sub>, the high dispersion of Pt particles and the high adsorption capacity of AlOOH to formaldehyde. Kim et al. [18] found that the Pt/TiO<sub>2</sub> catalyst prepared by reduction pretreatment, the oxygen consumption area on the catalyst surface was correlated with the proportion of Pt species, and the activated oxygen on the catalyst surface had impact on the activity of catalytic oxidation of formaldehyde. Cui et al. [19] found that acid-treated TiO<sub>2</sub> nanobelt supported platinum catalyst shows highly efficient activity for the catalytic oxidation of formaldehyde, due to the acid treated TiO<sub>2</sub> could possess more defect sites and more rougher surface and produce stronger interaction between Pt nanoparticles and hydroxyl species.

Furthermore, the size and dispersion of noble metal particles on the support are closely related to the activity of

catalytic oxidation of formaldehyde. Valden et al. [20] studied the influence of the size of gold nanoparticles on catalytic activity by using scanning tunnel (STM/STS) technique on Au/TiO<sub>2</sub> catalyst, they found that gold nanoparticles with non-metallic characteristic size (~3.5 nm) had the highest catalytic activity. In the Shen et al.'s work [21], it was found that the increase of Pd particle diameter led to the reduction of catalyst activity. The previous comparative experiments showed that [22], the Pt catalyst supported on TiO<sub>2</sub> had better catalytic oxidation activity than other carriers. TiO<sub>2</sub> not only had the excellent reducibility, but also had strong electron interaction with the active site [23], such as Qi et al. [24] used high-surface mesoporous Pt/TiO<sub>2</sub> hollow chains for efficient formaldehyde decomposition, the hollow chain-like structure, high specific surface area, numerous mesopores, and high volume of TiO<sub>2</sub> are main reasons for efficient formaldehyde oxidation. Furthermore, they synthesized hierarchically macro-/mesoporous Pt/TiO<sub>2</sub> catalyst for formaldehyde decomposition, the high catalytic activity is mainly attributed to hierarchically macro-/mesoporous structures of the TiO<sub>2</sub> support with large specific surface area and optimal pore size [25]. However, the low surface area was an obvious defect in the application of conventional TiO<sub>2</sub> as a catalytic carrier, which cannot guarantee the high dispersion of Pt nanoparticles in the loading process and cannot provide sufficient reaction space related to the adsorption or diffusion of reactants [26]. However, some researches [27, 28] showed that, adding different amounts of rare earth oxides can improve effectively the dispersion of supported noble metal catalysts and can make the particle size of active components become much smaller than that of unmodified ones, such as in the Shen et al.'s work [29], it was found that Pt/ZSM-5 through a facile nickel cation exhibits an excellent catalytic activity and stability for formaldehyde removal. Considering the high cost of precious metal Pt and low economic benefits, in this work, we use the commercial TiO<sub>2</sub> to support nano-Pt particles, and the rare earth metal Ce is doped to modify the defect of low activity of the catalyst. The loading of Pt in all of catalysts is controlled below 0.5%. The catalysts are prepared and explored their performance for the removal of formaldehyde with low concentration at room temperature.

## 2 Experimental

### 2.1 Catalyst Preparation

First, TiO<sub>2</sub> was modified by various amounts of Ce (0, 1, 5 and 7 wt%) by a impregnation method. For example, 0.279 g Ce(NO<sub>3</sub>)<sub>3</sub> was dissolved in a certain amount of deionized water and then under constant stirring 1.5 g TiO<sub>2</sub> was added to the Ce(NO<sub>3</sub>)<sub>3</sub> solution. After stirring

for 2 h, excess water was removed in a rotary evaporator at 80 °C. The samples were dried at 110 °C for 12 h and then calcined at 450 °C for 4 h. This catalyst was marked as x wt%Ce/TiO<sub>2</sub>. (x = 0, 1, 5 or 7).

Secondly, nano-Pt particles were loaded on Ce doped TiO<sub>2</sub> carrier by precipitation deposition method, and the Pt content of catalyst was 0.5%. Typically, 1.5 g x wt%Ce/TiO<sub>2</sub> was dissolved in 25 ml deionized water, and then a certain volume of H<sub>2</sub>PtCl<sub>6</sub> solution was added to the mixture and stir for 1 h. Then 0.1 mol/l NaOH solution was added to adjust ph to 10, aging at 60 C for 2 h under constant stirring. Subsequently, 2.5 ml 0.1 mol/l NaBH<sub>4</sub> solution was added to the mixture and stir for 0.5 h, the suspension was centrifuged and washed three times by deionized water, and then dried at 80 °C for 12 h. The final catalyst was denoted as 0.5% Pt-x wt% Ce/TiO<sub>2</sub> (x = 0, 1, 5 or 7).

## 2.2 Catalyst Characterization

The crystal structure of catalysts was analyzed by a MASAL XD-3 diffractometer (Beijing Purkinje Company). The test conditions were as follows: Cu K $\alpha$  ray ( $\lambda = 0.15406$  nm), tube voltage and tube current were 36 KV, and 20 mA respectively. Scanning speed was 8°/min. Scans were collected over a range of 2 $\theta$  from 0° to 80°.

Transmission electron microscope (TEM) and high angle dark field scanning transmission electron microscope (HAADF-STM) images were measured at 200 KV on a field emission transmission electron microscope Tecnai G2 F20 S-TWIN (FEI USA).

Micromeritics ASAP-2020 system was used to determine the N<sub>2</sub> adsorption–desorption isotherms of sample. Brunauer–Emmett–Teller (BET) method was used to calculate the specific surface area of samples, and Barrett–Joyner–Halenda (BJH) method was used to calculate the pore diameter distribution.

X-ray photoelectron spectroscopy (XPS) was performed using a multi-functional X-ray photoelectron spectrometer (Shimadzu Axis Ultra DLD, Kratos, UK). The spectra were obtained at ambient temperature. The binding energies were calibrated using the C1s peak of graphite at 284.6 eV as reference.

CO adsorption was measured on an AutoChem II2920 to analyze the Pt dispersion of the catalysts. Sample was firstly pretreated in hydrogen at 150 °C for 1 h and purged with helium for 1 h at the same temperature. And then, the catalyst was cooled to room temperature and CO pulses were injected from a calibrated online sampling valve. CO adsorption was assumed to be completed after three successive peaks showed the same peak areas. A CO/Pt stoichiometry of 1 was used for calculations.

## 2.3 Activity Test

Formaldehyde removal test was carried out in an organic glass sealed box (60 L) at room temperature, the wall of box was covered with a layer of aluminum foil and a free passage of air was created using a 5 W electric-fan. 200 mg catalysts were dispersed on a glass petri dish, which is placed at the bottom of catalytical reaction apparatus, covered with a glass slide; and formaldehyde detector was placed next to it. Before the test, 5  $\mu$ l solution including 37% formaldehyde solution was injected into the reactor and reached its gas phase equilibrium under the circulating fan flow.

The initial gas concentration of HCHO was controlled to keep  $20 \pm 2$  mg/m<sup>3</sup>, and then the glass cover was removed from dish and start the catalytic activity measurement.

## 3 Results and Discussion

### 3.1 Characterization of the Catalysts

The structural properties of TiO<sub>2</sub> and Pt supported catalysts were studied by X-ray diffraction characterization. Figure 1 shows that five diffraction peaks at  $2\theta = 25.3^\circ(101)$ ,  $37.8^\circ(004)$ ,  $48^\circ(200)$ ,  $53.9^\circ(105)$ ,  $55.1^\circ(211)$ , are typical for the anatase TiO<sub>2</sub> crystalline phase. Three diffraction peaks at  $2\theta = 27.5^\circ(110)$ ,  $36.1^\circ(101)$ ,  $41.2^\circ(111)$  belong to rutile crystalline phase. The diffraction peaks belonging to CeO<sub>2</sub> species are not observed in the diffraction patterns of modified TiO<sub>2</sub> and Pt-loaded catalyst. This indicates that CeO<sub>2</sub> species are highly dispersed on the surface of TiO<sub>2</sub>.

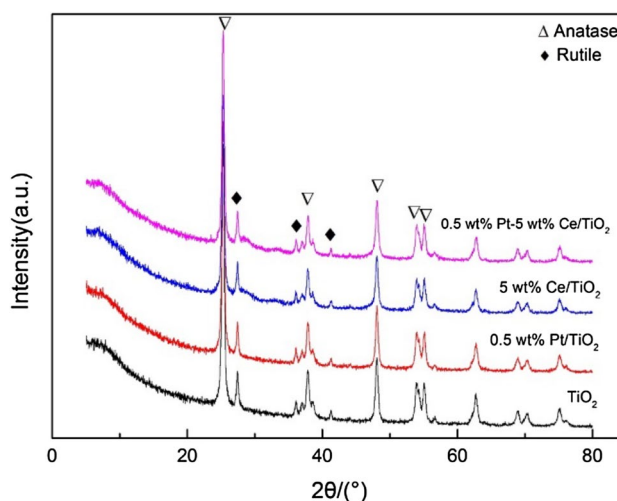
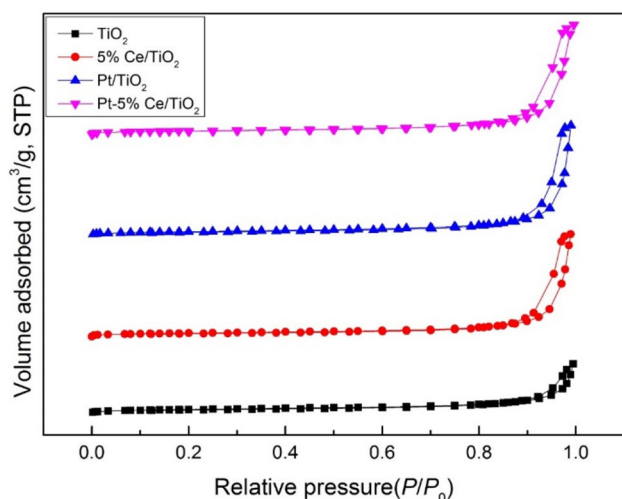


Fig. 1 Powder XRD patterns of TiO<sub>2</sub> and supported Pt catalysts

Moreover, there is no diffraction peak of Pt species on the Pt-loaded catalysts, reason is mainly the low Pt loading of (0.5 wt%) and the high dispersion of Pt nanoparticles on the supports, which is further confirmed in both Transmission Electron Microscopy and CO adsorption analysis.

To understand the physical properties of  $\text{TiO}_2$ , Pt-loaded catalysts and Ce doping catalysts,  $\text{N}_2$  adsorption–desorption isotherm of each sample is measured and analyzed in Fig. 2 and Table 1. All of the  $\text{N}_2$  adsorption isotherms show IV isotherm with H3 type hysteresis in the figure, this indicates that the sample possess a certain mesopores. Moreover, Table 1 shows that  $\text{TiO}_2$  has the maximum specific surface area of  $50 \text{ m}^2/\text{g}$ , and its surface area slightly decreases after doping 0.5 wt%Pt, whereas both  $S_{\text{BET}}$  of  $\text{TiO}_2$  drop to  $43 \text{ m}^2/\text{g}$  after modified by the Ce and Pt. The reason for decreasing of  $S_{\text{BET}}$  is that Pt and  $\text{CeO}_2$  particles enter into the pore of carrier and cause a blockage in it.

To explain the effect of Ce doping on the size and dispersion of Pt nanoparticles, TEM, STEM and CO adsorption characterization are performed to analyze Pt/ $\text{TiO}_2$  and



**Fig. 2**  $\text{N}_2$  adsorption–desorption isotherms of  $\text{TiO}_2$  and supported Pt catalysts

**Table 1** Physicochemical properties of  $\text{TiO}_2$  and supported Pt catalysts

Simple	$S_{\text{BET}}^{\text{a}}$ ( $\text{m}^2/\text{g}$ )	Pore volume ( $\text{cm}^3/\text{g}$ )	Pore size (nm)	Pt dispersion <sup>b</sup> (%)	Pt particle size <sup>c</sup> (nm)
Nano $\text{TiO}_2$	50	0.17	34.9	–	–
5 wt%Ce– $\text{TiO}_2$	43	0.36	21.2	–	–
Pt/ $\text{TiO}_2$	49	0.39	21.7	15.63	2.91
Pt/5 wt%Ce– $\text{TiO}_2$	43	0.35	21.4	45.33	2.21

<sup>a</sup>Calculated by BET method

<sup>b</sup>Calculated by CO adsorption

<sup>c</sup>Determined by TEM

Pt-5%Ce/ $\text{TiO}_2$  catalysts. The particle size of Pt is calculated by TEM and STEM images, showed in Figs. 3 and 4, and the degree of Pt dispersion is determined by CO adsorption characterization, listed in Table 1. Figures 3 and 4 show that Pt nanoparticles have no agglomeration and have high dispersion on the surface of supports. The average diameter of Pt particles in Pt/ $\text{TiO}_2$  catalyst is 2.91 nm, but the Pt diameter in Ce modified catalyst decreases to 2.2 nm. Furthermore, CO adsorption results show that the dispersion of Pt particles is significantly improved after the modification of Ce. All of characterizations indicated that Ce modification could stabilize Pt nanoparticles with small size and prevent agglomeration of Pt particles. A large amount of small Pt nanoparticles can increase the number of surface defects (ladders, borders, and corners), leading to exposure of active Pt nanoparticles on the catalyst surface. Thus, more active sites are provided for the oxidation reaction of formaldehyde at room temperature.

The important factors of HCHO oxidation at room temperature, as Huang et al. reported, were both the mobility of activated chemisorbed oxygen on the catalyst surface and the strong interaction between the support and precious metal [30]. The mobility of chemisorbed oxygen is more important to enhance the performance of catalyst than that of lattice oxygen. Furthermore, several previous works study demonstrated that the gas-phase oxygen could be dissociated and adsorbed at the oxygen vacancies, and could form the highly active species for the oxidation reaction [31]. Thus, in our work X-ray photoelectron spectroscopies of Pt/ $\text{TiO}_2$  and Pt-Ce/ $\text{TiO}_2$  catalysts are carried out to analyze the effect of Ce modification on the binding energies of Pt with O. Figure 7 shows that the binding energies between Pt 4f and O 1s, and the atomic radii of adsorbed O to lattice O are calculated by the XPS data of the modified and unmodified catalysts.

In Fig. 5, for the Pt/ $\text{TiO}_2$  and Pt-Ce/ $\text{TiO}_2$  catalysts, the binding energy peaks of Pt 4f<sub>7/2</sub> and Pt 4f<sub>5/2</sub> are found at 70.8/74.0 eV and 70.9/74.1 eV, respectively. Comparing with Pt 4f<sub>7/2</sub> standard binding energy of Pt<sup>0</sup>, Pt<sup>2+</sup> and Pt<sup>4+</sup> 71.1 and 72.4/74.2 eV, it indicates that there exist

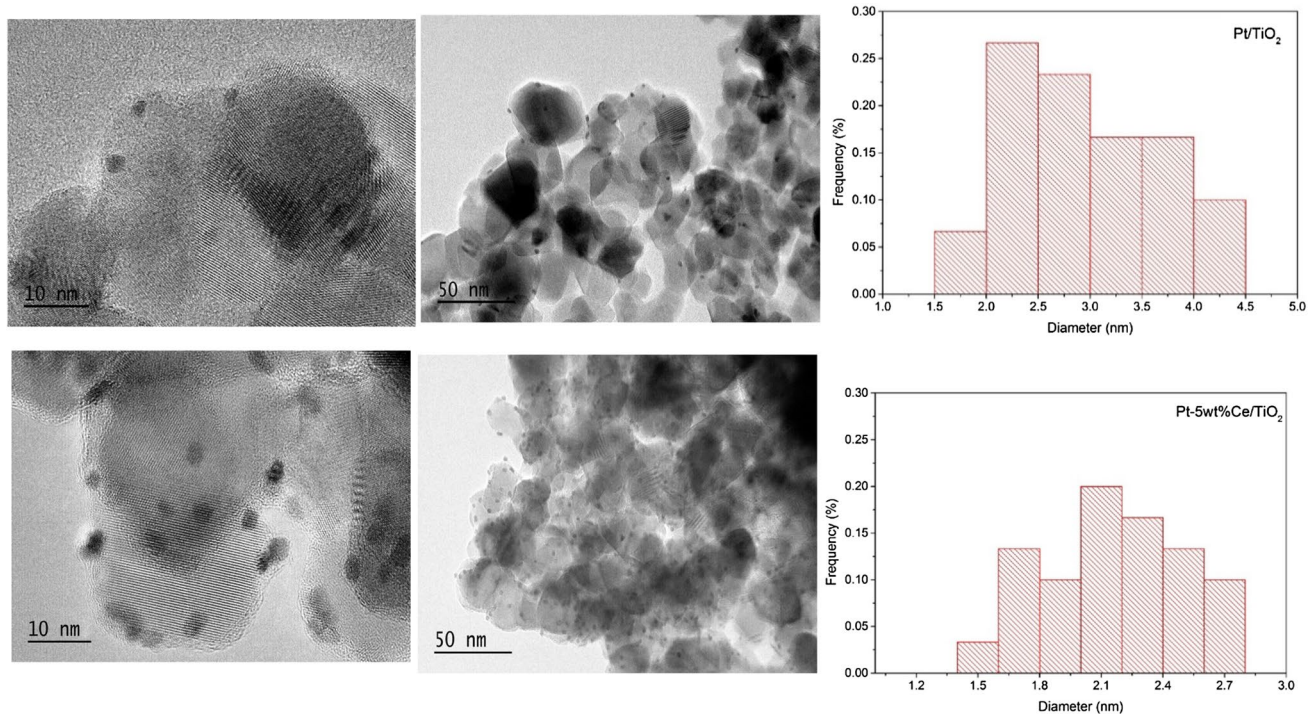


Fig. 3 TEM images of Pt/TiO<sub>2</sub> (1, 2) and Pt/5 wt% Ce–TiO<sub>2</sub> (3, 4) and their Pt particle size

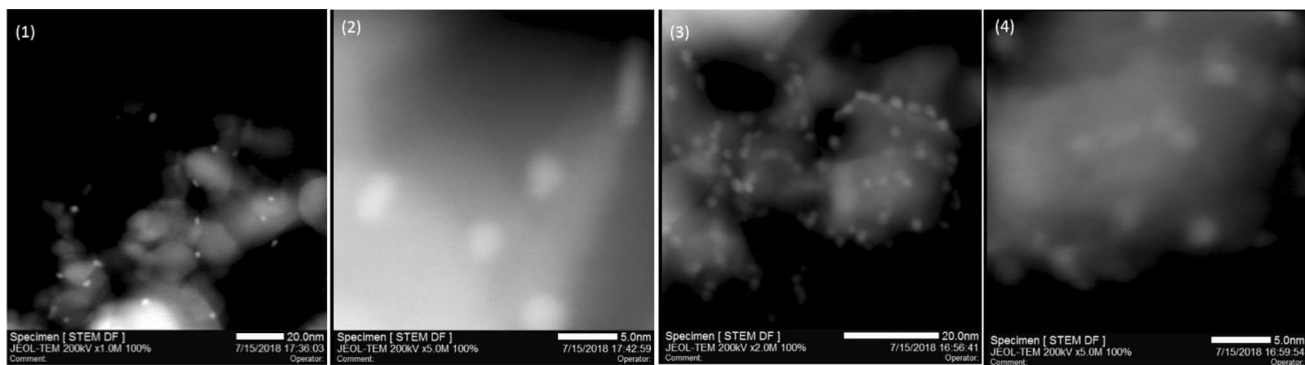


Fig. 4 HAADF-STEM images of Pt/TiO<sub>2</sub> (1, 2) and Pt/5 wt% Ce–TiO<sub>2</sub> (3, 4)

both Pt<sup>0</sup> and Pt<sup>4+</sup> in the catalysts. Moreover the incorporation of Ce makes the binding energy of Pt 4*f* go up 0.1 eV, and cause to the deviation of electron cloud of Pt. The peak area of Pt doped with Ce is much larger than that of unmodified Pt, leading to increasing of the number of electronegativity atoms in Pt microenvironment and further increasing of oxygen vacancy. It is consistent with the XPS data of O.

In the O 1*s* spectra of Pt/TiO<sub>2</sub> and Pt–Ce/TiO<sub>2</sub>, both the O 1*s* spectral lines can be divided into two peaks, one is the main peak of ~529.8 eV, which is mainly attributed to the lattice oxygen in TiO<sub>2</sub>, denoted as O<sub>lat</sub>, the other is shoulder

peak of ~530.8 eV, which is attributed to the chemical adsorption oxygen, denoted as O<sub>ads</sub>.

Compared with the O-1*s* spectra of unmodified Pt/TiO<sub>2</sub>, the O-1*s* peak of Pt–Ce/TiO<sub>2</sub> is wider, thus, the chemical bonds of atoms on the Pt–Ce/TiO<sub>2</sub> surface are unsaturated, and there are more oxygen vacancies. The SO<sub>ads</sub>/SO<sub>lat</sub> ratio are calculated by the peak area and listed in Table 2, it is found that SO<sub>ads</sub>/SO<sub>lat</sub> of modified Pt–Ce/TiO<sub>2</sub> is much larger than the unmodified Pt/TiO<sub>2</sub>. This is because CeO<sub>2</sub> has an incomparable oxygen storage capacity, which can provide a large number of oxygen vacancy and can promote the adsorption of oxygen to generate more O<sub>ads</sub>. Therefore

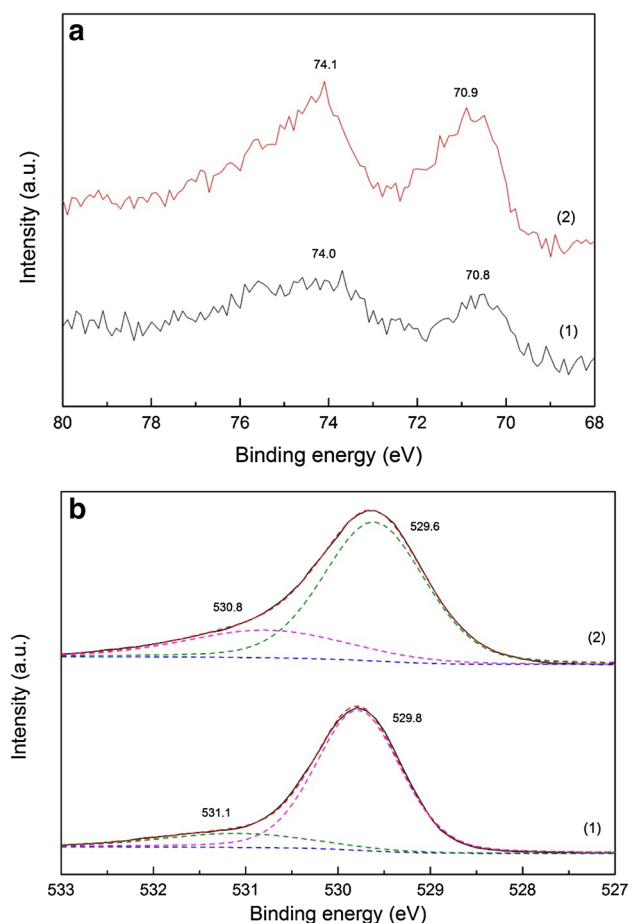


**Fig. 5** XPS analysis of Pt/TiO<sub>2</sub> (1) and Pt-5 wt% Ce/TiO<sub>2</sub> (2). **a** Pt 4f; **b** O 1s

the performance of Pt–Ce/TiO<sub>2</sub> catalyst is significantly enhanced after Ce doping.

### 3.2 Catalytic Activity

Figure 6 compares the activity of catalysts with different mass fraction of Ce doping (0%, 1%, 3%, 5%, 7%) by the residual and time curves of HCHO oxidation at room temperature. During the experiment, the error of HCHO detector is 1%. As shown in the Fig. 6, the catalytic performance of catalysts for formaldehyde oxidation has been improved whatever the ratio of Ce is used to modify. But the 5% Ce-doped catalyst possesses best catalytic activity. This Pt-5%Ce/TiO<sub>2</sub> catalyst could completely oxidize HCHO in the

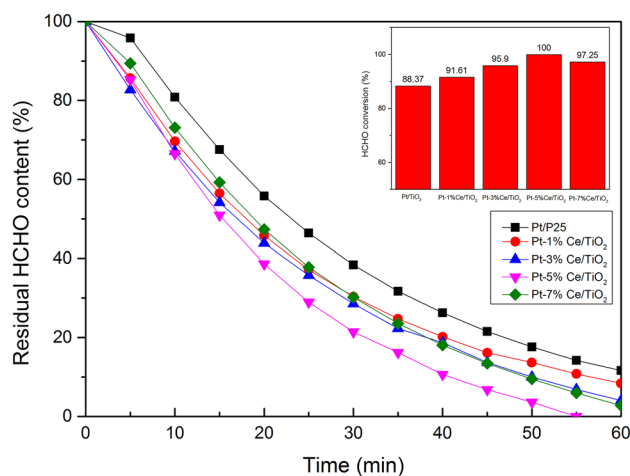


**Fig. 6** Activity of catalysts under different Ce doping amounts

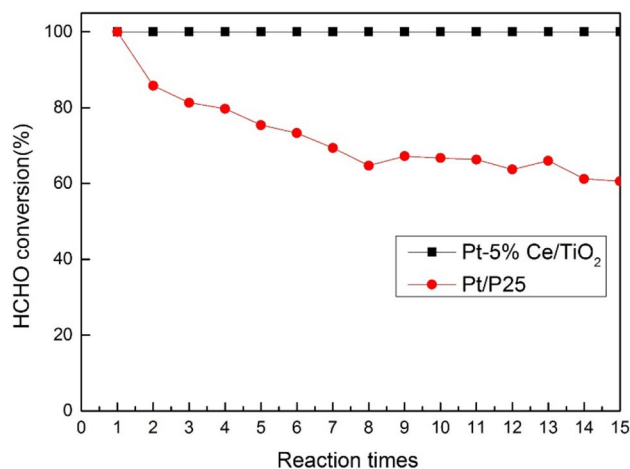


**Fig. 7** Catalytic performance of Pt/TiO<sub>2</sub> and Pt-5%Ce/TiO<sub>2</sub> and stability test for HCHO oxidation

reactor within 55 min. To test the stability of catalyst for HCHO oxidation, we set a 2-h reaction cycle and monitor the oxidation rate of HCHO in 15 cycles. As shown in Fig. 7, the Pt-5%Ce/TiO<sub>2</sub> catalyst could reach the oxidation rate of 100% in 15 cycles. The activity of Pt/TiO<sub>2</sub> catalyst rapidly decreased in the second cycle, because the active centers (Pt atom) of the catalyst start to deactivate. Thus, the catalysts after Ce doping exhibit stronger stability than unmodified catalysts.

**Table 2** XPS results of Pt/TiO<sub>2</sub> and Pt–Ce/TiO<sub>2</sub> catalysts

Sample	Pt 4f BE (eV)		Ti 2p BE (eV)	O 1s BE (eV)		SO <sub>ads</sub> /SO <sub>lat</sub>
	4f <sub>5/2</sub>	4f <sub>7/2</sub>		O <sub>ads</sub>	O <sub>lat</sub>	
Pt/TiO <sub>2</sub>	74.0	70.8	458.5	531.1	529.8	0.18
Pt/5 wt%Ce–TiO <sub>2</sub>	74.1	70.9	458.8	530.8	529.6	0.32

## 4 Conclusions

In this work, we report that the Ce modification can greatly improve the activity of Pt/TiO<sub>2</sub> catalyst for low concentration HCHO oxidation at room temperature as well as the stability of the catalyst. The catalyst with Ce doping amount of 5% possesses the best performance and can completely degrade the 20 mg/m<sup>3</sup> of HCHO in 55 min. After the catalyst is modified by Ce, the diameter of Pt nanoparticles would change from 2.9 to 2.2 nm, and the dispersion of Pt nanoparticles is enhanced by CO adsorption measurement. The addition of Ce can provide abundant oxygen vacancies on the catalyst surface, by the data of XPS characterization. This is conducive to chemisorb the oxygen from the air, and then promotes the catalytic oxidation of HCHO, leading to improvement of the activity of the catalyst. Therefore, the Pt/TiO<sub>2</sub> catalyst with the Ce doping possesses the excellent performance and a potential commercial value for removing low concentration of formaldehyde from indoor air.

**Acknowledgements** The authors gratefully acknowledge the financial support from National Natural Science Foundation of China (21676060 and 21676094), the Education Department of Guangdong province (2015KTSCX104), the Major projects of Guangzhou (201704020005), and the fundamental innovation research project of Guangzhou University (2017GDJC-M13).

## Compliance with Ethical Standards

**Conflict of interest** All authors declare that they have no conflict of interest.

## References

1. Conaway CC, Whysner J, Verna LK, Williams GM (1996) *Pharm Ther* 71(1–2):29–55
2. Li J, Li Z, Liu B, Xia Q, Xi HX (2008) *Chin J Chem Eng* 16(6):871–875
3. Liang WJ, Li J, Li JX, Zhu T, Jin YQ (2010) *J Hazard Mater* 175(1–3):1090
4. Zhang G, Xiong Q, Xu W, Guo S (2014) *Appl Clay Sci* 102:231–237

## Affiliations

Yuanyuan Shi<sup>1</sup>  · Zhiwei Qiao<sup>1</sup> · Zili Liu<sup>1</sup> · Jianliang Zuo<sup>1</sup>

Yuanyuan Shi  
867492350@qq.com

Zhiwei Qiao  
gzdxqzw@gmail.com

Jianliang Zuo  
gzdxzjl@gmail.com

5. Zhang G, Qin X (2013) *Mater Res Bull* 48:3743–3749
6. Sun H, Li J, Zhang G, Li N (2016) *J Mol Catal A-Chem* 424:311–322
7. An N, Wu P, Li S, Jia M, Zhang W (2013) *Appl Surf Sci* 285:805–809
8. Chen BB, Shi C, Crocker M, Wang Y, Zhu AM (2014) *Appl Catal B* 132–133(1):245–255
9. Zhang C, Liu F, Zhai Y, Ariga H, Yi N (2012) *Angew Chem* 51(28):8632–9628
10. Wang Z, Wang W, Zhang L, Jiang D (2016) *Catal Sci Technol* 6(11):3845–3853
11. Zhang C, Zhang J, Li Y, Wang L, He H (2015) *Catal Sci Technol* 5(4):2305–2313
12. Shen Y, Yang X, Wang Y, Zhang Y, Zhu H (2008) *Appl Catal B* 79(2):142–148
13. Zhou P, Yu J, Nie L, Jaroniec M (2015) *J Mater Chem A* 3(19):10432–10438
14. Zhang C, Li Y, Wang Y, He H (2014) *Environ Sci Technol* 48(10):5816
15. Chen D, Qu Z, Zhang W, Li X, Zhao Q (2011) *Colloids Surf A* 379(1):136–142
16. Sun X, Lin J, Guan H et al (2018) *Appl Catal B* 226:575–584
17. Yan Z, Xu Z, Yu J, Jaroniec M (2016) *Appl Catal B* 199:458–465
18. Kim GJ, Lee SM (2018) *RSC Adv* 9:3626
19. Cui W, Xue D, Yuan X et al (2017) *Appl Surf Sci* 411:105–112
20. Valden M, Lai X, Goodman DW (1998) *Science* 281(5383):1647–1650
21. Shen WJ, Kobayashi A, Ichihashi Y, Matsumura Y, Haruta M (2001) *Catal Lett* 73(2–4):161–165
22. Peng J, Wang S (2007) *Appl Catal B* 73(3–4):282–291
23. Tauster SJ, Fung SC, Garten RL (1978) *Chem Informationsdienst* 9(1):170–175
24. Qi L, Cheng B, Yu J et al (2016) *J Hazard Mater* 301:522–530
25. Qi L, Ho W, Wang J et al (2015) *Catal Sci Technol* 5(4):2366–2377
26. Mohamed AER, Rohani S (2011) *Energy Environ Sci* 4(4):1065–1086
27. Gaudet JR, Riva ADL, Peterson EJ, Bolin T, Datye AK (2013) *ACS Catal* 3(5):846–855
28. Wang F, Lu G (2008) *J Power Sources* 181(1):120–126
29. Junjie D, Zebao R, Pintian L et al (2018) *Appl Surf Sci* 457:670–675
30. Huang H, Leung DYC (2011) *ACS Catal* 1(4):348–354
31. Zhang C, He H (2007) *Catal Today* 126(3):345–350

**Publisher's Note** Springer Nature remains neutral with regard to jurisdictional claims in published maps and institutional affiliations.

<sup>1</sup> School of Chemistry and Chemical Engineering, Guangzhou University, Guangzhou, Guangdong, China